Risbridger, T., Watkins, D. W., Armstrong, J. P., Perriman, A., Anderson, J. L. R., & Fermin, D. J. (2016). Effect of Bioconjugation on the Reduction Potential of Heme Proteins. *Biomacromolecules*, *17*(11), 3485–3492. https://doi.org/10.1021/acs.biomac.6b00928

The Effect of Bioconjugation on the Reduction Potential of Heme Proteins

Thomas A.G. Risbridger[a], Dan W. Watkins[b], James P.K. Armstrong[c,d], Adam W. Perriman[c*], J.L. Ross Anderson[b*], David J. Fermin[a,*]

(a) School of Chemistry, University of Bristol, Bristol BS8 1TS, UK

(b) School of Biochemistry, University of Bristol, Bristol BS8 1TD, UK

(c) School of Cellular and Molecular Medicine, University of Bristol, Bristol BS8 1TD, UK

(d) Current affiliation: Department of Materials, Imperial College London, London SW7 2AZ, UK

ABSTRACT

The modification of protein surfaces employing cationic and anionic species enables the assembly of these bio-materials into highly sophisticated hierarchical structures. Such modifications can allow bioconjugates to retain or amplify their functionalities under conditions in which their native structure would be severely compromised. In this work, we assess the effect of this type of bioconjugation on the redox properties of two model heme proteins, i.e. cytochrome c (CytC) and myoglobin (Mb). In particular, the work focuses on the sequential modification by 3-dimethylamino propylamine (DMAPA) and 4-nonylphenyl 3-sulfopropyl ether (S1) anionic surfactant. Bioconjugation with DMAPA and S1 are the initial steps in the generation of pure liquid proteins, which remain active in the absence of water and up to temperatures above 150 C. Thin-layer spectroelectrochemistry reveals that DMAPA cationization leads to a distribution of bioconjugate structures featuring reduction potentials shifted up to 380 mV more negative than the native proteins. Analysis based on circular dichroism, MALDI-TOF mass spectrometry and zeta potential measurements suggest that the shift in the reduction potentials are not linked to protein denaturation, but to changes in the spin state of the heme. These alterations of the spin states originate from subtle structural changes induced by DMAPA attachment. Interestingly, electrostatic coupling of anionic surfactant S1 shifts the reduction potential closer to that of the native protein, demonstrating that the modifications of the heme electronic configuration are linked to surface charges.

Key-words: Bioconjugation; Cationization; Cytochrome c; Myoglobin; Spectroelectrochemistry; Reduction potential.

INTRODUCTION

Bioconjugation of proteins via cationization and electrostatic association of anionic polymer surfactants can lead to the generation of nearly dehydrated pure protein melt upon lyophilisation.[1] Myoglobin (Mb) has been the archetypal system for this type of modification, leading to an increase of 93°C in the decomposition temperature.[2] Indeed, pure myoglobin melts retain a higher percentage of secondary structure upon heating, with the capacity of refolding even after heating to temperatures of 155°C.[1d] Protein motions similar to those of fully hydrated proteins are retained in such materials. Typical native protein behaviour is therefore largely retained,[1c] with Mb melts continuing to exhibit reversible O_2 binding[2] and lipase melts exhibiting catalytic behaviour.[3]

Mb contains the iron-containing heme cofactor and has been shown previously to undergo direct electron transfer when adsorbed onto a graphite electrode pre-modified with a polymer surfactant[4] or polyelectrolyte.[5] Recently, it was shown that a Mb melt deposited onto highly oriented pyrolytic graphite (HOPG) showed quasi-reversible electrochemical behaviour,[6] and similar behaviour was exhibited up to 150°C on a gold electrode.[7] Little knowledge has been gathered about the redox properties of the protein prior to the lyophilisation step, which could provide information about changes in the environment near the heme. Indeed, the formal reduction potential of the heme is rather sensitive to its chemical environment, which has been a source of controversy in the literature.[8] The heme b cofactor is attached only *via* (non-covalent) proximal histidine ligation, and the distal site is not ligated by a protein-based residue. The spin states of native Mb can be affected by the ligating species in the distal position; the reduced deoxy form (deoxyMb) and water-ligated oxidised form (metMb) are high-spin while the O_2-bound reduced form is low spin.[9]

In contrast to Mb, cytochrome c (CytC) contains a heme c cofactor covalently bound to the protein *via* thio-ether linkages, and is ligated in the axial positions by histidine and methionine.[10] The sulfur in methionine is a strong-field ligand, and so native CytC is in a low-spin state for both Fe^{2+} and Fe^{3+} oxidation states close to physiological pH.[11] Although the heme group in both proteins shows a very well defined facile redox chemistry, the nature of the heme binding to the protein is rather different. Consequently, it could be expected that the surface modification could pose higher risk to the protein integrity in the case of Mb than CytC.

In this work, we provide a systematic study of the redox behaviour of CytC and Mb upon sequential modification by 3-dimethylamino propylamine (DMAPA) and nonylphenyl 3-sulfopropyl ether (S1) (illustrated in **Scheme 1**), employing thin-layer spectroelectrochemistry (SEC). We show that the protein cationization step generates a distribution of species that vary in the number of DMAPA modified residues and display a range of formal potentials shifted negatively by up to several hundred millivolts. In the case of Mb, the absorption spectra indicate that cationization induces a change of

high to low spin state, which is responsible for the shifts of the formal reduction potential. Cationization of CytC promotes the formation of the so-called alternate low spin state,[11a] which also manifests itself by a negative shift of the reduction potential. Binding of the anionic polymer surfactant S1 leads to a shift in the CytC bioconjugate formal potential closer to that of the native protein. In addition to the SEC responses, information obtained from circular dichroism, MALDI-TOF mass spectrometry, UV-Visible (UV-Vis) spectroscopy and zeta potential measurements clearly show that these substantial shifts in reduction potential are not related to protein denaturation, but rather to subtle changes in the heme Fe coordination.

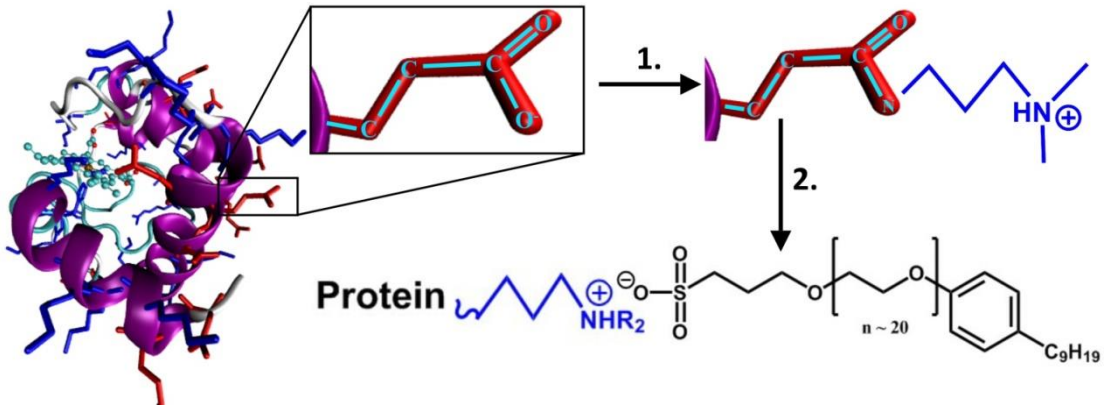

Scheme 1. Schematic diagram of CytC sequential bio-conjugation steps including 3-dimethylamino propylamine (DMAPA) coupling promoted by EDC (step 1.), followed by electrostatic adsorption of 4-nonylphenyl 3-sulfopropyl ether (S1) potassium salt (step 2.)

EXPERIMENTAL

Bioconjugate modification of Cytochrome c and Myoglobin. Cationization of CytC and Mb was achieved by a carbodiimide-activated condensation reaction to covalently attach 3-dimethylamino propylamine (DMAPA) molecules to acidic protein residues. Bioconjugation procedures followed those previously reported.[12] In brief, cationization involved addition of a 5 mg ml^{-1} aqueous solution of native protein to an aqueous solution of 0.65 M DMAPA adjusted to pH 6.5. Volumes used were calculated to give a large (50:1) excess of DMAPA per acidic residue. Solid N-(3-dimethylaminopropyl)-N-ethylcarbodiimide hydrochloride (EDC) was added to the solution in excess (20:1, EDC:acidic residue) with stirring over the course of an hour, and the pH was maintained at pH 6.0 – 6.5. The reaction was left to stir overnight. The resulting solution was dialysed against water for 24 hours and the purified cationized protein (cCytC or cMb) was freeze dried. The effect of bioconjugation in the presence of S1 was primarily assessed for cCytC. In this case, 3 $mgml^{-1}$ cCytC in pH 7.2 10 mM phosphate buffer were added to neat 4-nonylphenyl 3-sulfopropyl ether potassium salt

(S1) surfactant with stirring in the ratio 1:2 (positive charge:surfactant, assuming all acidic groups were cationized) and stirred overnight. The surfactant-conjugated product (S1cCytC) was purified by dialysing against pH 6.8 10 mM phosphate buffer for 24 hours.

Protein Characterization. Protein mass measurements before and after modification were determined by mass spectroscopy performed using an Applied Biosystems 4700 MALDI TOF/TOF mass spectrometer. UV-Vis spectra were obtained using a Perkin Elmer Lambda 25 spectrometer. Circular dichroism (CD) was measured using a Jasco J810 spectropolarimeter. Zeta potentials were measured using a Malvern instruments Zetasizer nano and analysed using Zetasizer software. Sample preparation followed standard procedures and is described in the supporting information.

Spectroelectrochemical analysis. Spectroelectrochemical (SEC) measurements were performed aerobically on protein solutions (typically 3 $mgml^{-1}$) prepared in 50 mM phosphate buffer (pH 7.5) containing 10% glycerol and 20 mM or 500 mM KCl. The redox mediators duroquinone (DQ), phenazine ethosulfate (PES), phenazine methosulfate (PMS), 1,2-Naphthoquinone (NQ) and 2,3,5,6-Tetramethylphenylenediamine (DAD) were added. Solutions were added to a thin layer cell (0.3 mm) set up for UV-Vis and electrochemical measurements. To minimise redox state equilibration times, small sample volumes were used. This was achieved by first adding the sample solution containing glycerol to the thin layer cell, followed by careful addition of a second electrolyte solution containing no glycerol or sample. Mixing was prevented by the difference in viscosity of the two layers. Ionic conduction occurs across the liquid interface, allowing reference (KCl saturated. Ag/AgCl) and counter (Pt) electrodes to be placed in the larger volume of second solution as shown in **Figure S1**. A Pt gauze working electrode (WE) was inserted into the thin layer cell. UV-Vis spectra were recorded at set intervals using an Agilent Technologies Cary-60 spectrometer, and the periodically stepped potential of the WE was applied by a Biologic SP-150 potentiostat. Spectra were recorded upon stepping the potential from positive to negative values (forward direction) and back to the initial potential (backward direction). All reduction potentials are reported vs standard hydrogen potential (SHE), based on a value of $E_{Ag/AgCl}$ = 0.200 vs SHE at room temperature (ignoring the contribution associated with the H_2 partial pressure). Further experimental information including chemicals used, protein modification and characterization and (spectro)electrochemical analysis can be found in the supporting information (**Section S1** and **S2**).

RESULTS AND DISCUSSION

Spectroelectrochemical responses upon conjugation of Mb and CytC. Figure 1 shows the evolution of the UV-Vis spectra as a function of the applied potential of native CytC and the two modified forms, cationized (cCytC) and bioconjugated (S1cCytC). In the case of CytC, spectra

associated with completely oxidised and reduced forms (reported in **Figure S2**) are obtained in the range of 0.365 to 0.015 V vs SHE.[13] CytC spectra shows a clear isosbestic point at 408 nm, which is consistent with the evolution from a single molecular species to another. In the cases of cCytC and S1cCytC, the potential range had to be expanded to between 0.455 and -0.295 V, while the isosbestic point is less clearly defined than in the case of the native protein. Additional small peaks are observed in the spectra of S1cCytC, including a shoulder at 389 nm (due to the phenazine methosulfate mediator) and peaks at 560 and 613 nm. These observations suggest that bioconjugation leads to a range of structures with different reduction potentials.

Nernst curves, fraction of the reduced heme as a function of the applied potential, generated from the SEC data are shown in **Figure 2**. Absorbance values were selected at the wavelength exhibiting the greatest change in absorption upon redox state change (typically at 414nm). Such values were measured at a range of applied potentials, normalised and recorded as the fraction of protein in the reduced state. For each protein variant, the response exhibited essentially no hysteresis on the timescale of the measurement (30 mins for CytC, 60 mins for cCytC and S1cCytC). **Figure S3** shows a similar analysis for cCytC in the Q-band range (550 nm), revealing similar behaviour to the one in **Figure 2A**. The native protein follows a shape consistent with a one electron transfer with a single midpoint potential occurring at 0.24 V vs SHE, similar to literature values.[14] Although the onset potential for heme reduction in cCytC and S1cCytC is close to the one observed for the native CytC, it is clear that changes in the population of the reduced heme extend over a larger potential range. In the case of Mb (**Figure 2B**), cationization of the protein also leads to a substantial shift of the reduction potential towards a more negative (and broader) potential range. The corresponding normalized spectra at the various electrode potentials are shown in **Figure S4**. Native Mb is characterized by a single potential Nernst curve at 0.04 V, which is close to values reported in the literature.[15] This behaviour further suggests that bioconjugation leads to a range of protein with different extent of modification, including a population of native-like protein.

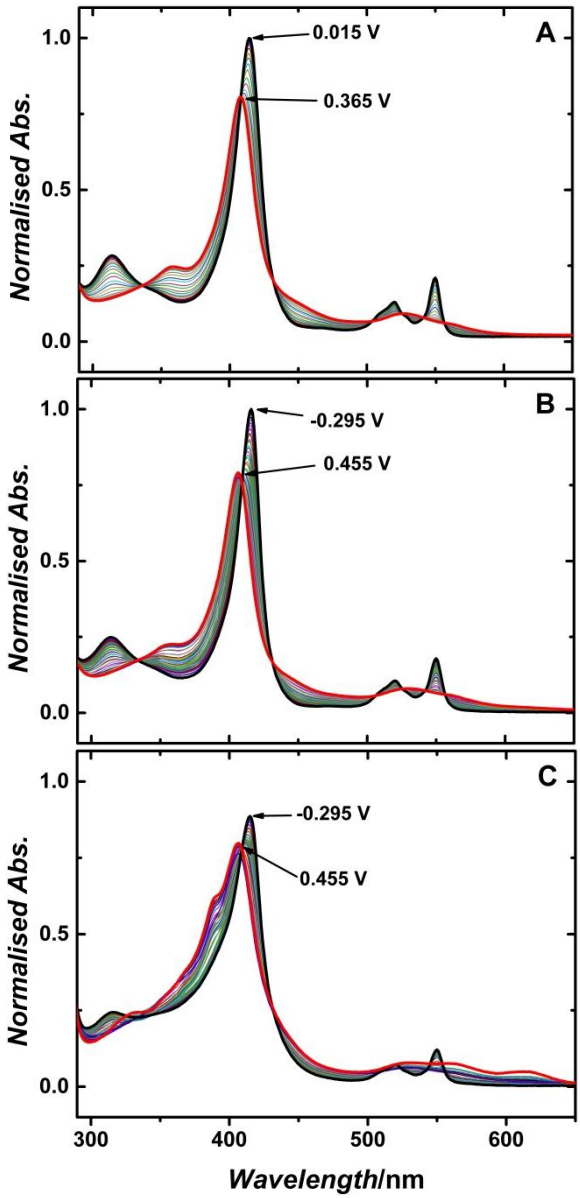

Figure 1. UV-Vis spectra of 3 mg ml^{-1} of CytC (A), cCytC (B) and S1cCytC (C) in pH 7.5 electrolyte containing 50 mM phosphate buffer, 500 mM KCl and 10% glycerol. The redox mediators used added to the electrolyte include duroquinone, phenazine ethosulfate, phenazine methosulfate, 1,2-Naphthoquinone and 2,3,5,6-Tetramethylphenylene-diamine. Each spectra was recorded after a 30 or 60 min equilibration period (for native and modified protein respectively) at each potential. In the case of CytC, the potential was varied between 0.015 to 0.365 V, while spectral changes for the bioconjugate were examined between -0.295 and 0.455 V. Note that peak at 389 nm in (C) is caused by phenazine methosulfate mediator.

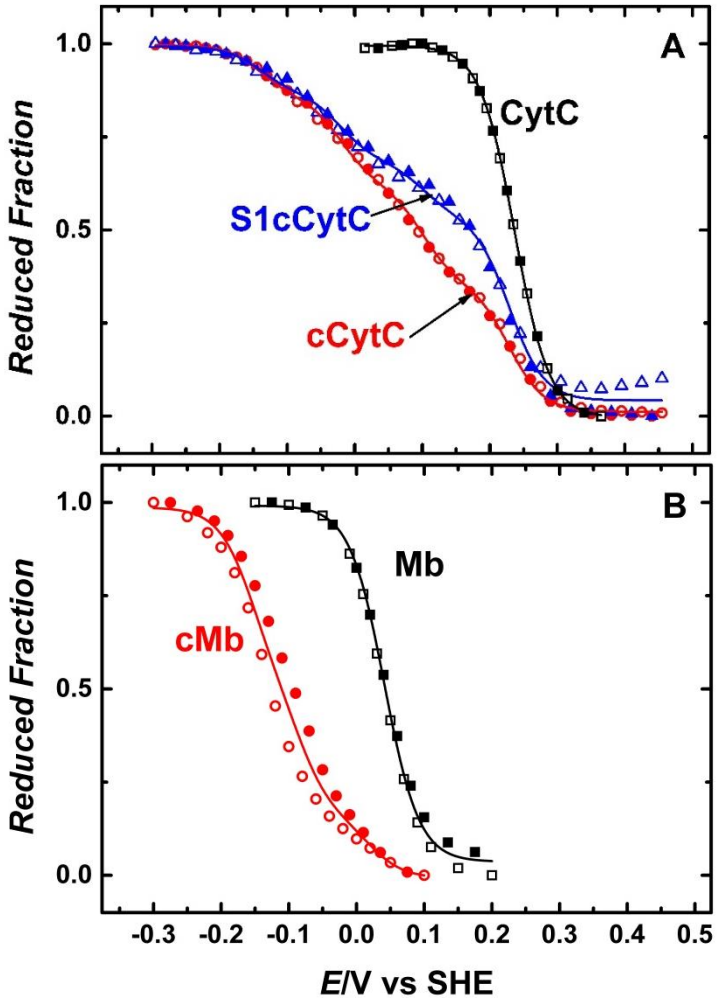

Figure 2. Changes in the fraction of reduced heme as a function of potential in the case of CytC (A) and Mb (B). Substantial modification in the redox behaviour can be observed between native (black), cationized (red) and surfactant modified conjugates (blue). For native protein, each data point (electrode potential) was measured after 30 minutes equilibration time, while conjugates were allowed to equilibrate for 60 minutes. The electrode potential was initially stepped towards negative values (forward direction, full symbols), followed by sequential steps towards the initial potential (backward direction, open symbols). The fact that the trend strongly overlap between forward and backward directions indicate that the system reached redox equilibrium at each potential. Solid lines represent fitting to the Nernst equation (see supporting information). The composition of the electrolyte solutions is as indicated in the caption of **Figure 1.**

The complex Nernst behaviour observed for the bioconjugates can be rationalized in terms of a distribution of species with discrete reduction potentials. As discussed in the supporting information (**Section S2** and **Figure S5**), the behaviour of CytC conjugates can be accurately reproduced by

considering four different species each representing a discrete redox species. The relative population and formal reduction potential of the various species obtained by linear least square fitting of the Nernst plot for CytC and Mb are summarised in **Table 1**. The data shows that the formal reduction potential of approximately 1/3 cCytC species is affected very little by the protein modification, with the remaining population showing potential displacements between -50 to -380 mV. Upon attachment of S1, the effective speciation of the bioconjugate shifts towards the C1 product, i.e. the species with the reduction potential closer to the native CytC. Following the same procedure, the Nernst curves for the cMb were fitted considering three main species. Contrary to the case of CytC, the highest population corresponds to the species with the largest shift in the reduction potential (M3). Indeed, the Nernst curve for cMb does not show a substantial broadening in the potential range as seen in CytC, but rather a large shift to more negative potential. Interestingly, there is a more significant hysteresis in the case of cMb, suggesting a reduced electron transfer rate as discussed in the supporting information. We propose that this is caused by greater physical rearrangement at the iron centre upon reduction/oxidation than occurs for native Mb. The effect of S1 modification in the case of Mb is complicated by the possibility of heme loss under forcing oxidizing conditions,[8a, 8d, 16] thus we shall restrict our discussion to only the cationization step.

Table 1. Speciation, relative abundancy (fraction) and formal potentials obtained from fitting the spectro-electrochemical data in **Figure 2** to three- and four-species variants of **Equation S3** for CytC and Mb respectively. Values are for native and modified CytC and Mb measured in 50 mM phosphate buffer in 500 mM KCl.

Protein	Speciation	E°’ / V	($E^\circ - E_{Native}^\circ$) / V	Population after DMAPA	Population after S1
CytC	**C1**	0.23	-0.01	0.34	0.50
	C2	0.19	-0.05	0.27	0.15
	C3	-0.02	-0.26	0.24	0.19
	C4	-0.14	-0.38	0.14	0.12
Mb	**M1**	0.02	-0.02	0.17	-
	M2	-0.08	-0.12	0.38	-
	M3	-0.16	-0.20	0.45	-

The underlying assumption in this analysis is that the population of non-modified protein is negligible, thus species C1 and M1 represent a population of cationized protein in which DMAPA exerts a minor effect on the reduction potential of the heme. We have also fitted the Nernst curves assuming that the reduction potentials of C1 and M1 are identical to the corresponding native protein. Although the quality of the fits are slightly poorer, the results are not statistically different to those shown on table 1. However, as discussed further below, MALDI-TOF analysis conclusively show that the population of un-modified protein is not consistent with those estimated from the SEC analysis. On the other hand, statistical analysis of the Nernst curve of S1cCytC bioconjugate does not provide any clear evidence of changes in the reduction potential of the various species resulting from the cationization steps. Consequently, we conclude that the magnitude in the shift of the reduction potential upon cationization is determined by the position of the specific acid residue modified by DMAPA, while the effect of the S1 attachment on the redox responses is only significant for those species in which DMAPA is bound close to the heme moiety.

Similar experiments were conducted in the absence of mediators as described in the supporting information (**Section S3**). The target of these studies is to assess whether the apparent shift in formal potentials is related to specific interactions with the selected redox mediators. **Figure S6** shows a well-defined Nernstian curve for CytC, similar to the responses shown in **Figure 2A**. The mediator-less responses for cCytC and S1cCytC are also characterised by a significant broadening of the potential range consistent with the complex speciation observed in the presence of the mediators. However, a significant level of hysteresis is observed between the forward and backward traces, suggesting a significant decrease in the direct electron transfer rate constant to the heme moiety. Furthermore, **Figure S7A** compares cyclic voltammograms of CytC, cCytC and S1cCytC in solution. While the native protein does exhibit a clear redox response associated with the heme, only background capacitive current are seen for the bioconjugates in the same potential range. On the other hand, no clear faradaic responses are observed for either Mb or cMb in solution (**Figure S7B**). These results show that, except for the native CytC, direct electron transfer to the heme moieties is strongly hindered.

Bioconjugation of CytC. Changes in the heme formal reduction potential as a result of modification of the protein structure have been widely investigated,[17] and can arise from a variety of structural aspects.[18] A trivial explanation for our experimental observations could involve protein denaturation, however the analysis described below provide conclusive evidences that this is not the case.

The absorption spectra of native CytC, cCytC and S1cCytC are reported in **Figure 3A**. The data show subtle spectral changes upon cationization, suggesting changes in the heme environment. In particular, the Soret band is blue-shifted by 2 nm and the absorbance of the charge transfer (CT) band at 695 nm decreases. The heme cofactor in native CytC is bis-ligated by histidine and methionine, promoting a low spin-state configuration. Changes from low to high spin-states have been previously observed under mild-denaturing conditions,[19] leading to a displacement of the Soret band to 395 nm and positive shifts in the formal potential.[20] Such changes are inconsistent with the behaviour observed upon cationization of CytC, indicating that the heme remains in the low spin-state. The band observed at 695 nm is characteristic of the methionine-sulfur:heme-iron axial complexation;[21] loss of this feature indicates that methionine is no longer binding. However, the retention of low-spin character indicates axial binding by an alternative strong-field ligand such as an amine-based residue[11a] or hydroxide species.[22] Mugnol *et al*.[11a] reported the formation of the so-called alternate low spin-state upon micellar encapsulation of CytC which exhibited a -200 mV shift in formal potential with respect to the free protein. This was accompanied by UV-Vis spectral changes similar to those observed upon cationization, suggesting that a similar alternate low spin-state is generated in DMAPA modified CytC. Alternative low spin-state CytC was also shown to exhibit a decrease in rhombic symmetry by electron paramagnetic resonance measurements consistent with a ligand shift, and to have a more open heme crevice compared to the normal low-spin state CytC. Further spectral changes are observed for S1cCytC, and a more pronounced splitting is observed in the CT-band. This may indicate that some fraction of S1cCytC is in a reduced state under the conditions of this measurement.

MALDI-TOF MS measurements of the native and bioconjugated CytC are displayed in **Figure 3B.** The cationization step resulted in a broad distribution of m/z values equivalent to a mass increase of 186 – 1260 Da from the highest intensity native CytC signal. The highest abundancy material has a mass increase equivalent to attachment of 8 DMAPA molecules. Interestingly, the discrete peaks around the maximum of the distribution (inset in **Figure 3B**) correspond to integer amounts of DMAPA moieties (84 Da), with at least six clearly identifiable species, the fractional distribution of which are shown in **Figure S8**. This distribution does not closely follow the fractional speciation reported in **table 1**, suggesting that the observed shifts in reduction potential are caused by modification of specific residues rather than by incremental changes in positive charges. The mass spectrum of S1cCytC is very similar to that of cCytC, except for a more pronounced tail at higher m/z values. This behaviour suggests that the S1 binding is rather weak, leading to detachment of the surfactant upon ionization. MALDI-TOF MS was measured below 1000 Da for CytC and cCytC after silver sulfate treatment to cleave thio-ether bonds in heme c,[23] as shown in **Figure S9**. No change in heme mass occurred upon cationization, indicating that no covalent attachment of DMAPA to acidic propionate groups took

place. Such a chemical change to the heme group is expected to directly influence reduction potential. A similar analysis of cMb also concluded that DMAPA does not directly bind to the heme moiety.

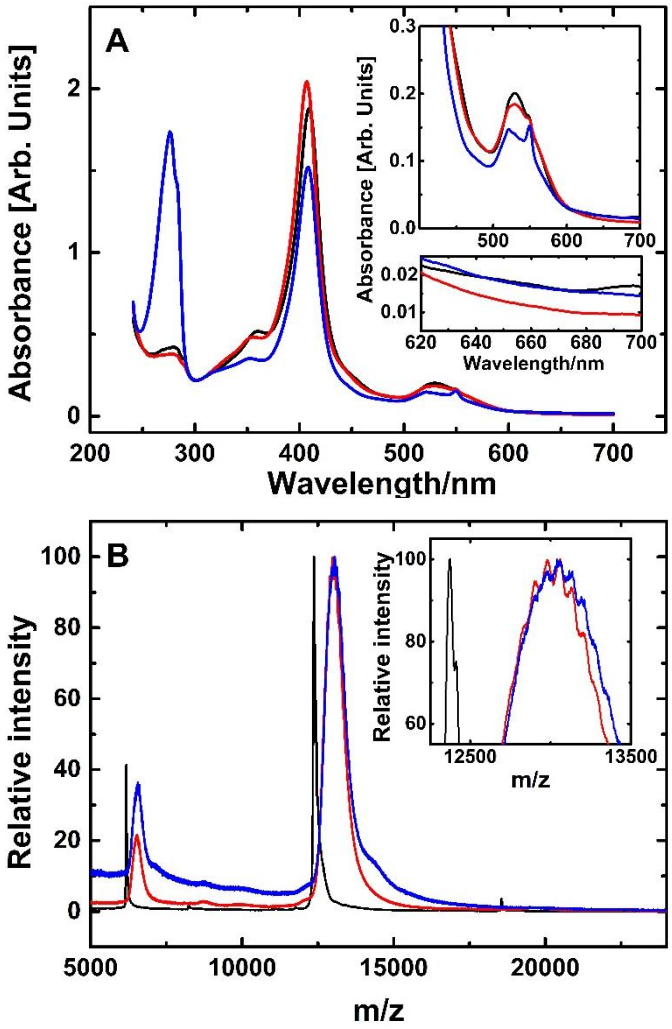

Figure 3. UV-Vis spectra (A) and MALDI-TOF mass spectra (B) of the native CytC (black line), cCytC (red line) and S1cCytC (blue line). Protein concentration for UV-Vis was 0.3 mg ml^{-1} in pH 7.2 10 mM phosphate buffer, under no-potentiostatic control. The continuing presence of a large peak at 276 nm in the S1cCytC spectrum after extensive product dialysis confirms attachment of S1. MS shows both singly and doubly charged molecular ions, inset shows that the molecular ion is made up of a distribution of overlapping peaks, with differences between adjacent peaks close to the 84 Da expected upon each attachment of DMAPA through the condensation type reaction.

The attachment of DMAPA clearly manifests itself by an increase in zeta potential values as shown in **Figure 4A**. Subsequent attachment of anionic S1 generates bioconjugate with a negative

charge at all pH due to the characteristic charge overcompensation seen in electrostatic layer-by-layer assembly. However, the S1cCytC zeta potential dependence is rather unusual, showing a decrease in the absolute charge at pH close to neutrality. This behavior suggests a complex balance of electrostatic and hydrophobic interactions in the bio-conjugate which requires further investigation. **Figure 4B** compares the circular dichroism (CD) spectra of the native CytC and bioconjugates at pH 7.5. Slight changes in the ratio of the 208 and 222 nm peaks can be taken as evidence of modifications in the secondary structure upon cationization. However, the ratio of these two peaks is restored to the values corresponding to native CytC upon attachment of S1. Further evidences for the partial recovery of the native CytC structure upon attachment of S1 are given by SEC responses in lower ionic strength electrolyte, favouring stronger electrostatic S1 attachment, as displayed in **Figure S10**. While the Nernst curves for CytC and cCytC are little affected by the decreasing the concentration of KCl from 500 mM to 20 mM, the trend for S1cCytC approaches closer to that observed for the native protein (see also **Table S1**). We additionally report that a liquid-protein melt was produced by lyophilisation and subsequent heating of S1cCytC at 40°C as shown in figure s11, and that this protein phase was similar in appearance to that which has previously been reported for solvent-free Mb melts.[1d]

Cationization of Mb. The MALDI-TOF MS and UV-Vis spectra corresponding to Mb and cMb are reported in **Figure 5A**. A mass increase of between 294 – 2815 Da is observed upon cationization, with the highest abundancy species exhibiting a mass increase equivalent to binding of 18 DMAPA molecules. We note that the reported mass distributions for both cCytC and cMb include some values higher than expected assuming complete cationic modification of all acidic residues in the native proteins. This may indicate the presence of non-specifically bound DMAPA in some of the modified protein. Zeta potential measurements have previously shown that cationization of Mb increases the zeta potential by at least +20 mV.[2, 24] In the case of Mb, cationization has a large effect upon the secondary structure due to changes in electrostatic stabilization and the disruption of internal salt bridges, and CD spectra for this have been reported elsewhere.[1d] These changes in the secondary structure have a strong effect on the heme environment which manifests itself by red shifts in the Soret and changes in the shape of the Q-bands as shown in **Figure 5B**. These spectral changes are consistent with a shift to low spin-state iron in the heme moiety (**Figure S12**).[25] However, the observed spectral changes and circular dichroism spectroscopy previously reported[1d] for myoglobin clearly indicate that the cationization process does not lead to protein denaturation.

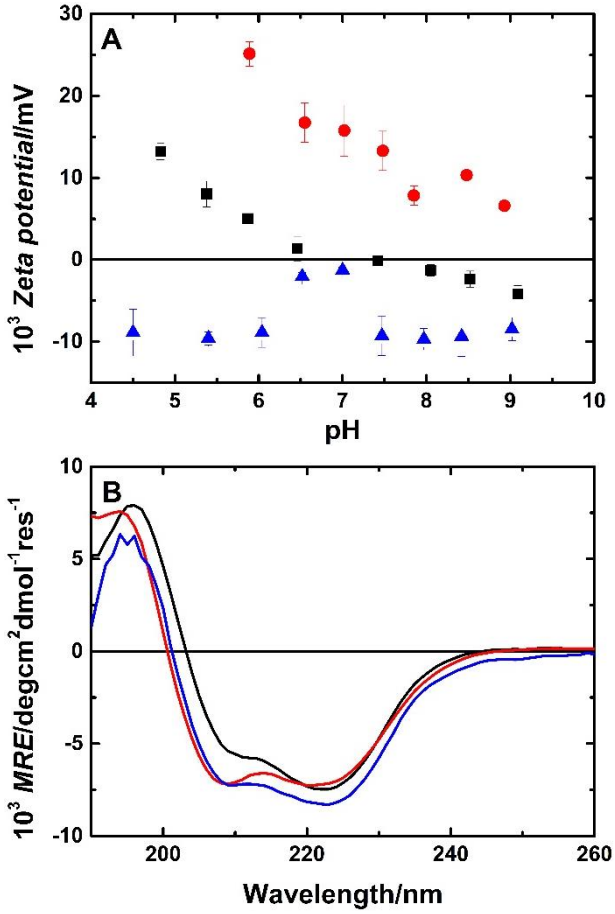

Figure 4. Zeta potential as a function of pH (A) and CD spectra (B) in 20 mM phosphate buffer, pH 7.5 at 22°C for CytC (black), cCytC (red) and S1cCytC (blue).

Heme b in native myoglobin is ligated by histidine in the proximal position, but has a free distal position available for O_2 binding. Previously, the binding of a water molecule in this position has been suggested as the cause of the spectral shift,[1d] on the basis of spectral changes seen in Mb mutants at high pH.[26] However, this water binding is unlikely to alter the Fe spin-state. Feng *et al*.[27] have shown that imidazole ligation in this site generates a field strong enough to promote the transition in spin-state, which also manifests itself by a significant shift of the formal potential towards negative values. Additionally, UV/Vis spectra reported by Nakanishi *et al.* for Mb-mutants incorporating bis-histidine ligated heme show remarkable similarity to those reported here in figure 5b and S12 for reduced cMb.[28] Consequently, we suggest that the cationization step promotes the movement of a nearby histidine residue closer to the heme, allowing it to ligate in the distal position. However, we note that O_2 is a strong-field ligand which would also promote a high- to low- spin transition upon binding to cMb-heme. Although the reduced and oxidized spectra of cMb (Figure S12) are distinct from that expected for oxyMb reported for example by Schenkman *et al*.,[29] recent work by Armstrong *et al.* has

shown that surfactant bound cationized Mb is able to bind oxygen, and releases bound oxygen only under conditions of extreme hypoxia.[24] Consequently, we cannot entirely exclude the possibility that O_2 could be binding a population of reduced cMb, although this expected to be small given the hindered diffusion configuration characteristic of thin-layer cells.

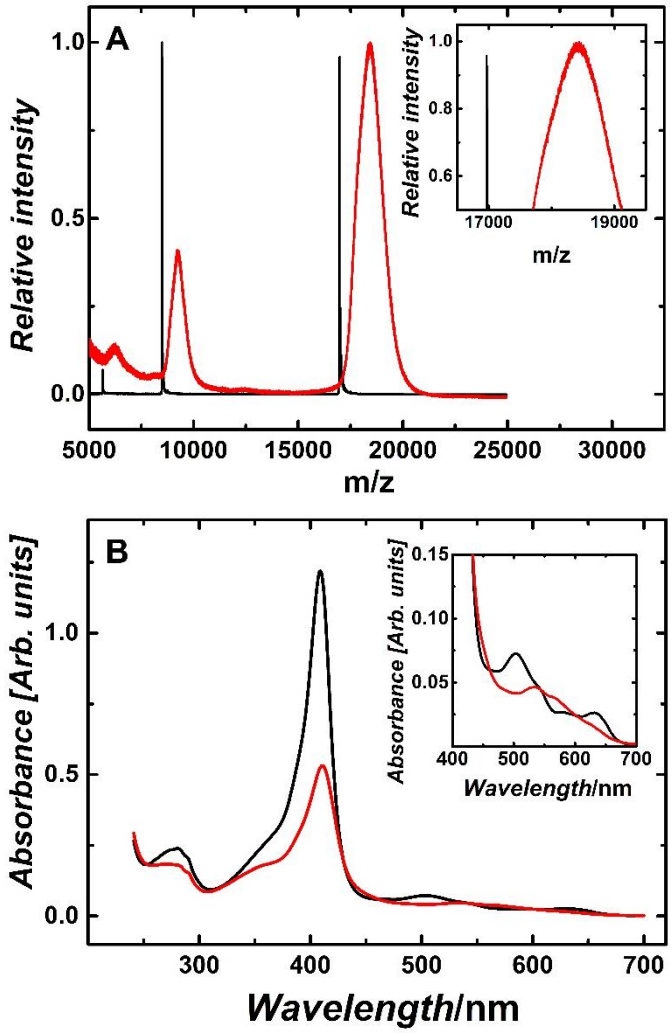

Figure 5. MALDI-TOF MS (A) and UV-Vis spectra of native Mb (black line) and cMb (red line). Both singly and doubly charged protein peaks are shown in MS, and a large product distribution of cationized products are generated. UV-Vis spectra measured in pH 6.8 20 mM phosphate buffer.

CONCLUSIONS

The present study demonstrates the highly sensitive nature of the reduction potential of heme proteins to controlled attachment of charged species. We specifically observed that covalent

attachment of DMAPA to CytC and Mb generates a distribution of species with different numbers of cationized residues, which manifests itself by a distribution of reduction potential. The speciation of the cationized proteins was assessed by employing thin-layer spectroelectrochemistry, identifying species with reduction potentials shifted by values as large as -0.38 V. Changes in the overall charge of the bioconjugate were confirmed by zeta potential measurements, while MALDI-TOF analysis confirmed the strong link of DMAPA to the protein. Importantly, the observed spectral changes and circular dichroism spectroscopy shown here for cytochrome c, and previously for myoglobin,[2] clearly indicate that the bioconjugation process does not lead to protein denaturation.

The changes in redox responses revealed two contrasting situations for Mb and CytC bioconjugates. In the case of Mb, DMAPA binding results in a change from high to low Fe spin-state. We propose that structural changes induced by DMAPA allow the nearby histidine residue to coordinate the available distal position of the Fe centre. The observed SEC changes in CytC are consistent with a shift to the so-called alternate low-spin state, and may also result from a change in heme-iron ligation. Interestingly, the overall negative shift of the reduction potential is compensated to an extent by the attachment of S1. Although zeta potential measurements show a charge overcompensation, a population of proteins exhibiting the alternate low-spin state remains.

In principle, speciation analysis based on SEC analysis can lead to a quantitative approach to specific interactions between redox protein and charged molecules. While techniques such as mass spectrometry and zeta potential measurements provide accurate information on the extent of molecular attachment, SEC is sensitive to changes occurring in the vicinity of the heme. Some of these structural changes may lead to strongly hindered direct electron transfer processes, as demonstrated in this work. However, carefully chosen redox mediators allow the reduction potential of these complex distribution of species to be probed.

Associated Content

Supporting Information Available

The Supporting Information is available free of charge on the ACS Publications website at DOI: xxxxxx.

Additional experimental details including sample preparation for protein characterization and thio-ether cleavage for CytC heme analysis, **Figures S1 – S12 and Table S1** as referred to in the text, spectroelectrochemistry, mediator-less spectroelectrochemistry, cyclic voltammograms of native and modified proteins in solution.

Acknowledgments

The authors would like to thank Alain R. P. Santiago for helpful discussion. This work was supported by funding from the Leverhulme Trust (Grant RPG-2013-103). We thank the Elizabeth Blackwell Institute for funding JPKA and EPSRC (Early Career Fellowship EP/K026720/1) for support of AWP. JLRA is grateful for the University Research Fellowship funded by the Royal Society. DJF acknowledges the support by the Institute of Advanced Studies of the University of Bristol (University Research Fellowship).

References

1. (a) Perriman, A. W.; Colfen, H.; Hughes, R. W.; Barrie, C. L.; Mann, S., Solvent-Free Protein Liquids and Liquid Crystals. *Angew. Chem., Int. Ed.* **2009,** *48* (34), 6242-6246; (b) Perriman, A. W.; Mann, S., Liquid Proteins-A New Frontier for Biomolecule-Based Nanoscience. *ACS Nano* **2011,** *5* (8), 6085-6091; (c) Gallat, F. X.; Brogan, A. P. S.; Fichou, Y.; McGrath, N.; Moulin, M.; Hartlein, M.; Combet, J.; Wuttke, J.; Mann, S.; Zaccai, G.; Jackson, C. J.; Perriman, A. W.; Weik, M., A Polymer Surfactant Corona Dynamically Replaces Water in Solvent-Free Protein Liquids and Ensures Macromolecular Flexibility and Activity. *J. Am. Chem. Soc.* **2012,** *134* (32), 13168-13171; (d) Brogan, A. P. S.; Siligardi, G.; Hussain, R.; Perriman, A. W.; Mann, S., Hyper-thermal stability and unprecedented re-folding of solvent-free liquid myoglobin. *Chem. Sci.* **2012,** *3* (6), 1839-1846.
2. Perriman, A. W.; Brogan, A. P. S.; Colfen, H.; Tsoureas, N.; Owen, G. R.; Mann, S., Reversible dioxygen binding in solvent-free liquid myoglobin. *Nat. Chem.* **2010,** *2* (8), 622-626.
3. Brogan, A. P. S.; Sharma, K. P.; Perriman, A. W.; Mann, S., Enzyme activity in liquid lipase melts as a step towards solvent-free biology at 150 degrees C. *Nat. Commun.* **2014,** 5:5058.
4. Nassar, A. E. F.; Zhang, Z.; Hu, N. F.; Rusling, J. F.; Kumosinski, T. F., Proton-coupled electron transfer from electrodes to myoglobin in ordered biomembrane-like films. *J. Phys. Chem. B* **1997,** *101* (12), 2224-2231.
5. Ma, H. Y.; Hu, N. F.; Rusling, J. F., Electroactive myoglobin films grown layer-by-layer with poly(styrenesulfonate) on pyrolytic graphite electrodes. *Langmuir* **2000,** *16* (11), 4969-4975.
6. Sharma, K. P.; Bradley, K.; Brogan, A. P. S.; Mann, S.; Perriman, A. W.; Fermin, D. J., Redox Transitions in an Electrolyte-Free Myoglobin Fluid. *J. Am. Chem. Soc.* **2013,** *135* (49), 18311-18314.
7. Sharma, K. P.; Risbridger, T.; Bradley, K.; Perriman, A. W.; Fermin, D. J.; Mann, S., High-Temperature Electrochemistry of a Solvent-Free Myoglobin Melt. *ChemElectroChem* **2015**, 976-981.
8. (a) de Groot, M. T.; Merkx, M.; Koper, M. T. M., Heme release in myoglobin-DDAB films and its role in electrochemical NO reduction. *J. Am. Chem. Soc.* **2005,** *127* (46), 16224-16232; (b) Guto, P. M.; Rusling, J. F., Myoglobin retains iron heme and near-native conformation in DDAB films prepared from pH 5 to 7 dispersions. *Electrochem. Commun.* **2006,** *8* (3), 455-459; (c) de Groot, M. T.; Merkx, M.; Koper, M. T. M., Additional evidence for heme release in myoglobin-DDAB films on pyrolitic graphite. *Electrochem. Commun.* **2006,** *8* (6), 999-1004; (d) de Groot, M. T.; Merkx, M.; Koper, M. T. M., Evidence for heme release in layer-by-layer assemblies of myoglobin and polystyrenesulfonate on pyrolitic graphite. *J. Biol. Inorg. Chem.* **2007,** *12* (6), 761-766.
9. (a) Adams, K. L.; Tsoi, S.; Yan, J. S.; Durbin, S. M.; Ramdas, A. K.; Cramer, W. A.; Sturhahn, W.; Alp, E. E.; Schulz, C., Fe vibrational Spectroscopy of myoglobin and cytochrome f. *J. Phys. Chem. B* **2006,** *110* (1), 530-536; (b) Makinen, M. W.; Churg, A. K.; Glick, H. A., Fe-O_2 Bonding and Oxyheme Structure in Myoglobin. *Proc. Natl. Acad. Sci. U. S. A.* **1978,** *75* (5), 2291-2295.
10. Bushnell, G. W.; Louie, G. V.; Brayer, G. D., High-Resolution 3-Dimensional Structure of Horse Heart Cytochrome-C. *J. Mol. Biol.* **1990,** *214* (2), 585-595.
11. (a) Mugnol, K. C. U.; Ando, R. A.; Nagayasu, R. Y.; Faljoni-Alario, A.; Brochsztain, S.; Santos, P. S.; Nascimento, O. R.; Nantes, I. L., Spectroscopic, structural, and functional characterization of the alternative low-spin state of horse heart cytochrome c. *Biophys. J.* **2008,** *94* (10), 4066-4077; (b) Loehr,

T. M.; Loehr, J. S., Determination of Oxidation and Spin States of Heme Iron - Resonance Raman Spectroscopy of Cytochrome c, Microperoxidase, and Horseradish-Peroxidase. *Biochem. Biophys. Res. Commun.* **1973,** *55* (1), 218-223; (c) Yamamoto T.; Palmer G.; Gill D.; Salmeen I. T.; L., R., The Valence and Spin State of Iron in Oxyhemoglobin as Inferred from Resonance Raman Spectroscopy. *J. Biol. Chem.* **1973,** *248*, 5211-5213.

12. Sharma, K. P.; Collins, A. M.; Perriman, A. W.; Mann, S., Enzymatically Active Self-Standing Protein-Polymer Surfactant Films Prepared by Hierarchical Self-Assembly. *Adv. Mater.* **2013,** *25* (14), 2005-2010.

13. Wang, L.; Santos, E.; Schenk, D.; Rabago-Smith, M., Kinetics and Mechanistic Studies on the Reaction between Cytochrome c and Tea Catechins. *Antioxidants* **2014,** *3* (3), 559.

14. (a) O'Reilly, N. J.; Magner, E., Electrochemistry of cytochrome c in aqueous and mixed solvent solutions: Thermodynamics, kinetics, and the effect of solvent dielectric constant. *Langmuir* **2005,** *21* (3), 1009-1014; (b) Battistuzzi, G.; Borsari, M.; Cowan, J. A.; Ranieri, A.; Sola, M., Control of cytochrome c redox potential: Axial ligation and protein environment effects. *J. Am. Chem. Soc.* **2002,** *124* (19), 5315-5324.

15. Brunori, M.; Saggese, U.; Rotilio, G. C.; Antonini, E.; Wyman, J., Redox Equilibrium of Sperm-Whale Myoglobin, Aplysia Myoglobin, and Chironomus-Thummi Hemoglobin. *Biochemistry* **1971,** *10* (9), 1604-1609.

16. (a) Hargrove, M. S.; Krzywda, S.; Wilkinson, A. J.; Dou, Y.; Ikedasaito, M.; Olson, J. S., Stability of Myoglobin - a Model for the Folding of Heme-Proteins. *Biochemistry* **1994,** *33* (39), 11767-11775; (b) Hargrove, M. S.; Singleton, E. W.; Quillin, M. L.; Ortiz, L. A.; Phillips, G. N.; Olson, J. S.; Mathews, A. J., His(64)(E7)-]Tyr Apomyoglobin as a Reagent for Measuring Rates of Hemin Dissociation. *J. Biol. Chem.* **1994,** *269* (6), 4207-4214.

17. (a) Mauk, A. G.; Moore, G. R., Control of metalloprotein redox potentials: What does site-directed mutagenesis of hemoproteins tell us? *J. Biol. Inorg. Chem.* **1997,** *2* (1), 119-125; (b) Battistuzzi, G.; Borsari, M.; Dallari, D.; Lancellotti, I.; Sola, M., Anion binding to mitochondrial cytochromes c studied through electrochemistry - Effects of the neutralization of surface charges on the redox potential. *Eur. J. Biochem.* **1996,** *241* (1), 208-214; (c) Rees, D. C., Experimental Evaluation of the Effective Dielectric-Constant of Proteins. *J. Mol. Biol.* **1980,** *141* (3), 323-326; (d) Bhagi-Damodaran, A.; Petrik, I. D.; Marshall, N. M.; Robinson, H.; Lu, Y., Systematic Tuning of Heme Redox Potentials and Its Effects on O_2 Reduction Rates in a Designed Oxidase in Myoglobin. *J. Am. Chem. Soc.* **2014,** *136* (34), 11882-11885; (e) Costa, C.; Moore, G. R., The effect of surface charge on the reduction potential and heme propionate ionization of a monoheme cytochrome: spectroscopic and potentiometric studies of trifluoroacetylated cytochrome c(551) from Pseudomonas aeruginosa. *Inorg. Chim. Acta* **1998,** *276* (1-2), 256-262; (f) Olson, T. L.; Williams, J. C.; Allen, J. P., Influence of protein interactions on oxidation/reduction midpoint potentials of cofactors in natural and de novo metalloproteins. *Biochim. Biophys. Acta, Bioenerg.* **2013,** *1827* (8-9), 914-922; (g) Bendall, D. S., *Protein Electron Transfer*. Bios Scientific: Oxford, 1996.

18. Moore, G. R.; Pettigrew, G. W.; Rogers, N. K., Factors Influencing Redox Potentials of Electron-Transfer Proteins. *Proc. Natl. Acad. Sci. U. S. A.* **1986,** *83* (14), 4998-4999.

19. Gebicka, L.; Gebicki, J. L., Kinetic studies on the interaction of ferricytochrome c with anionic surfactants. *J. Protein. Chem.* **1999,** *18* (2), 165-172.

20. Fedurco, M.; Augustynski, J.; Indiani, C.; Smulevich, G.; Antalik, M.; Bano, M.; Sedlak, E.; Glascock, M. C.; Dawson, J. H., The heme iron coordination of unfolded ferric and ferrous cytochrome c in neutral and acidic urea solutions. Spectroscopic and electrochemical studies. *Biochim. Biophys. Acta, Proteins Proteomics* **2004,** *1703* (1), 31-41.

21. Brautigan, D. L.; Feinberg, B. A.; Hoffman, B. M.; Margoliash, E.; Peisach, J.; Blumberg, W. E., Multiple Low-Spin Forms of Cytochrome-c Ferrihemochrome - Epr-Spectra of Various Eukaryotic and Prokaryotic Cytochromes-c. *J. Biol. Chem.* **1977,** *252* (2), 574-582.

22. Silkstone, G. G.; Cooper, C. E.; Svistunenko, D.; Wilson, M. T., EPR and optical spectroscopic studies of Met80X mutants of yeast ferricytochrome c. models for intermediates in the alkaline transition. *J. Am. Chem. Soc.* **2005,** *127* (1), 92-99.
23. Fisher, W. R.; Taniuchi, H.; Anfinsen, C. B., Role of Heme in Formation of Structure of Cytochrome-C. *J. Biol. Chem.* **1973,** *248* (9), 3188-3195.
24. Armstrong, J. P. K.; Shakur, R.; Horne, J. P.; Dickinson, S. C.; Armstrong, C. T.; Lau, K.; Kadiwala, J.; Lowe, R.; Seddon, A.; Mann, S.; Anderson, J. L. R.; Perriman, A. W.; Hollander, A. P., Artificial membrane-binding proteins stimulate oxygenation of stem cells during engineering of large cartilage tissue. *Nat. Commun.* **2015,** *6:7405*
25. Boffi, A.; Das, T. K.; della Longa, S.; Spagnuolo, C.; Rousseau, D. L., Pentacoordinate hemin derivatives in sodium dodecyl sulfate micelles: Model systems for the assignment of the fifth ligand in ferric heme proteins. *Biophys. J.* **1999,** *77* (2), 1143-1149.
26. Ikedasaito, M.; Hori, H.; Andersson, L. A.; Prince, R. C.; Pickering, I. J.; George, G. N.; Sanders, C. R.; Lutz, R. S.; Mckelvey, E. J.; Mattera, R., Coordination Structure of the Ferric Heme Iron in Engineered Distal Histidine Myoglobin Mutants. *J. Biol. Chem.* **1992,** *267* (32), 22843-22852.
27. Feng, M. L.; Tachikawa, H., Raman spectroscopic and electrochemical characterization of myoglobin thin film: Implication of the role of histidine 64 for fast heterogeneous electron transfer. *J. Am. Chem. Soc.* **2001,** *123* (13), 3013-3020.
28. Nakanishi, N.; Takeuchi, F.; Park, S. Y.; Hori, H.; Kiyota, K.; Uno, T.; Tsubaki, M., Characterization of heme-coordinating histidyl residues of an engineered six-coordinated myoglobin mutant based on the reactivity with diethylpyrocarbonate, mass spectrometry, and electron paramagnetic resonance spectroscopy. *J. Biosci. Bioeng.* **2008,** *105* (6), 604-613.
29. Schenkman, K. A.; Marble, D. R.; Burns, D. H.; Feigl, E. O., Myoglobin oxygen dissociation by multiwavelength spectroscopy. *J. Appl. Physiol.* **1997,** *82* (1), 86-92.

TOC

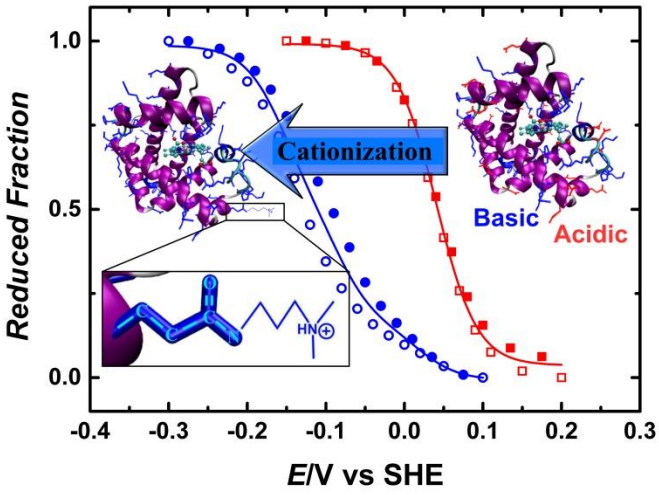
Reduced Fraction
1.0
0.5
0.0
-0.4
-0.3
-0.2
-0.1
0.0
0.1
0.2
0.3
E/V vs SHE
Cationization
Basic
Acidic
HN